Short Communication

Development of a New Point of Care Testing for Electrochemical Detection of Glucose in Blood

Hui Wang[1] and Kun Wang*

[1] General Medicine, Liaoning Cancer Hospital and Institute, Shenyang, Liaoning 110041, China
[2] Obstetrics and Gynecology, Peace Branch of Northern Theatre General Hospital, Shenyang, Liaoning 110812, China
*E-mail: wangkgood@163.com

Currently, blood glucose testing in the hospital is performed by an automated biochemistry analyzer in the laboratory and the point of care testing (POCT) meter. In this work, a POCT meter was fabricated with Pt-Pd nanowires. Combined with electrochemical synthesis techniques, an enzyme-free electrochemical sensor for glucose detection was constructed with a porous anodic alumina template with Pt-Pd standing on a gold electrode surface. Optimal conditions were determined in this work for glucose detection and also the sensitivity, stability, repeatability and interference resistance of the sensor for glucose detection were examined under simulated physiological conditions. In addition, the proposed POCT electrochemical sensor was adopted to compare the results with those of a biochemical instrument.

1. INTRODUCTION

With the aging of the population, diabetes has become the third major disease after malignant tumors and cardiovascular diseases. It is one of the world's most serious public health problems that threaten human health. Diabetes is a lifelong metabolic disease, which is not fatal, but the complications resulted from it can be life-threatening [1–3]. Blood glucose testing is essential for determining whether a diabetic's blood glucose control is up to standard [4,5]. Through accurate blood glucose testing, clinicians can understand the specific circumstances that led to the increase or decrease of blood glucose in the patients. Blood glucose testing also helps doctors accurately assess the extent of glucose metabolism disorders in diabetic patients and develop appropriate treatment plans [6–8]. Currently, blood glucose testing in the hospital is performed by an automated biochemistry analyzer in the laboratory and the point of care testing (POCT) meter [9–12].

Using biochemical analyzers to measure venous plasma or serum glucose concentrations is the preferred method for clinical glucose testing, for it is scientifically accurate and easily influenced by the external environment, and the influencing factors are easily controlled [13–16]. However, it is not suitable for a long-term testing for patients due to its long testing time as well as the complicated operation and procedure. With the advantages of convenience, speed and simple operation, the POCT blood glucose meter has been widely applied in clinical and patient's home [17–19]. The POCT blood glucose test can keep tracking the changes of patients' blood glucose, thus the treatment plan can be adjusted in time to reduce the complications caused by poor blood glucose control and improve the quality of life of patients. POCT blood glucose testing has become a new trend in the future development of laboratory medicine and has received an increasing attention [20–23]. However, since POCT blood glucose meters are mostly adopted to measure peripheral whole blood glucose values of patients, they are susceptible to the effects of humidity and temperature [20,22,24,25]. They are also easily affected by the performance of the instrument and the proficiency of the operation. In this work, Pt-Pd nanowire arrays were prepared by electrodeposition of Pt and Pd alloys on anodic aluminum oxide (AAO) film, which were installed on screen-printed electrode substrates. This POCT sensor has a fast electron transfer rate and mass transfer rate, as well as a high electrocatalytic oxidation performance for glucose. It was used to compare the results with those of a biochemical instrument and the results show that the stability of the POCT sensor can be applied to practical assays.

2. EXPERIMENTAL

2.1 Materials and instruments

All reagents were analytical grade and applied without further purification. Anodized aluminum oxide porous template (AAO template) was purchased from Shanghai Chaowei Nanotechnology Co. The conductive carbon paste was purchased from Atchison Corporation, USA. The conductive silver paste was purchased from Shanghai Bao Yin Electronic Materials Co. The polyester screen was purchased from Shanghai Yuanhang Screen Printing Equipment Co. The deposition precursor solution was prepared with 5 mM K_2PtCl_4 + 5 mM $(NH_4)_2PdCl_4$ + 0.2 M H_3BO_3.

The screen printing machine (LC-500) was purchased from Shanghai NetYi Silk Screen Printing Ink Co. The vacuum vaporizer (JEC-1600) was purchased from JEOL Japan Electronics. The electrochemical workstation (CHI600) was from Shanghai Chenhua Instruments Co.

2.2 Preparation of Pt-Pd/Au POCT sensor

The preparation of the screen-printed Au electrode consists of two parts: the conductive and insulating layers were prepared by a screen printer, and the Au layer was atomically ejected in the working area by means of a vacuum vaporizer. Specifically, the silver paste ink was printed through the stencil onto the PVC substrate as the conductive layer, and dried in a 40° oven for 0.5 h. The polymeric insulating ink was covered with another stencil to form the insulating layer and dried in a 40° oven for

0.5 h. Finally, a working area with a diameter of 3 mm was left to cover the rest of the electrode. The electrodes were gold sprayed for 10 min with a vacuum vaporizer, and dried in a 40° oven for 15 min to obtain Au film electrodes with a thickness of about 200 nm.

The AAO-Au electrode was fabricated by electrosputtering a gold film of about 200 nm on the back side of the AAO template with a vacuum vapor deposition apparatus, and the AAO template with the gold film on the back side was glued to the electrode by double-sided conductive adhesive for subsequent electrodeposition.

Electrodeposition was performed in three electrodes with AAO-Au electrode being the working electrode, Pt wire being the counter electrode and saturated Ag/AgCl being the reference electrode. First, the AAO-Au electrode was immersed in the precursor solution. To allow the precursor solution to fully enter the pores of AAO, the system was evacuated for 20 min before electrodeposition. The deposition potential was -0.1 V and the electrodeposition time was 15 min. During the deposition, the precursor solution was stirred with a magnetic stirrer to obtain uniformly sized nanowire arrays. After the electrodeposition, the electrode surface was cleaned with ultrapure water to remove the residual precursor solution. Subsequently, the electrode was immersed in 1 M NaOH solution for 30 min to remove the AAO. The final electrode was denoted as Pt-Pd/Au.

3. RESULTS AND DISCUSSION

The SEM image of Pt-Pd nanowires is shown in Figure 1A. At low deposition potentials, the precursor fluid can be filled into the pores of AAO in time for relatively slow electrical reduction of Pt and Pd ions. The SEM images show that the prepared nanowire arrays are uniformly upright on the surface of the Au electrodes [26], with a relatively uniform distribution of diameters. They have no agglomerative collapse, and their shapes and diameters are consistent with the AAO pore channels [27].
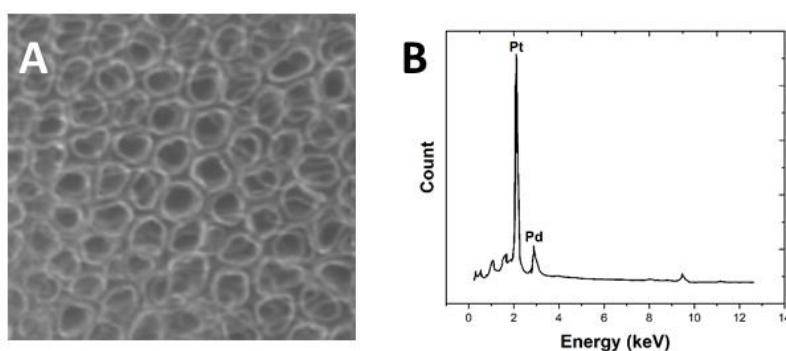
Figure 1. (A) SEM image and (B) EDX spectrum of Pt-Pd nanowires.

Figure 1B shows the EDX energy spectrum of the sample. It can be found that the EDX provides significant diffraction peaks of Pt and Pd. The diffraction peaks of Pt are around 2 keV and 10 keV and the diffraction peaks of Pd are around 3 keV and 11 keV. The above results prove that Pt and Pd have been Figure 1B shows the EDX energy spectrum of the sample. It can be found that the EDX provides

significant diffraction peaks of Pt and Pd. The diffraction peaks of Pt are around 2 keV and 10 keV and the diffraction peaks of Pd are around 3 keV and 11 keV. The above results prove that Pt and Pd have been successfully deposited on Au electrodes by constant potential deposition [28]. No diffraction peaks of Au were found in the energy spectrum, thus it can be assumed that the array is completely covered on the electrode surface [29].

At present, glucose sensors are mainly applied in blood glucose detection. Therefore, considering its practical application, this study investigated the electrocatalytic oxidation of glucose by Pt-Pd/Au in physiomimetic solution (0.1 M PBS, pH 7.4). Figure 2 shows the cyclic voltammetric behavior of Pt-Pd/Au before and after the addition of 10 mM glucose (sweep potential window of -0.6~1 V, sweep rate of 30 mV/s). It can be noted from the CV diagram that after the addition of glucose, there are obvious oxidation peaks around the three potentials of -0.4V, 0.2V and 0.6V, the reason for which is the multi-electron transfer oxidation of glucose on the Pt-Pd surface, indicating that Pt-Pd/Au can effectively catalyze the electrooxidation of glucose [30–32].
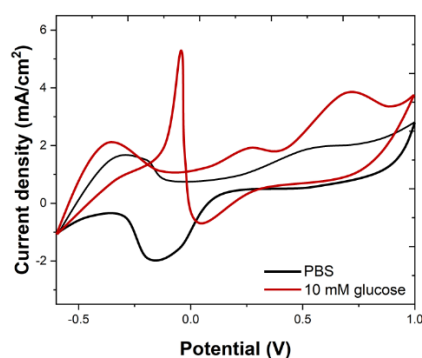
Figure 2. CV of Pt-Pd/Au in the 0.1 M PBS (pH: 7.4) with the presence and absence of 10 mM glucose.
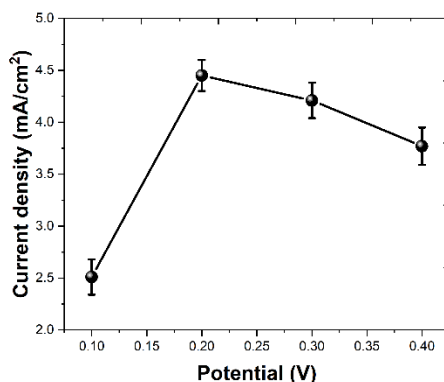
Figure 3. Chronoamperometric response of the Pt-Pd/Au upon 10 mM glucose obtained at different potential.

To obtain the best detection results, the relationship between the amperometric response of Pt-Pd/Au and the detection potential were investigated, with the results shown in Figure 3. The time-current method was performed by injecting 10 mM glucose into 0.1 M PBS at 0.1 V, 0.2 V, 0.3 V and 0.4 V,

and averaging the values after three measurements at each potential. It was found that the sensor had the most sensitive amperometric response at a level of 0.2V. Therefore, 0.2V was selected as the subsequent detection potential.

The chronoamperometric assay was performed by adding a certain concentration of glucose solution to 0.1 M PBS solution at 0.2 V potential every 30 s and the results are shown in Figure 4A, which reveals that when a certain concentration of glucose is added to the PBS solution, the current suddenly increases in a stepwise manner and then reaches a stable plateau. The short time required for the current to reach a stable state indicates that the sensor has a fast response capability [33–35].

The plots of Pt-Pd/Au sensor for glucose concentration are presented in Figure 4B. It can be seen that the current density of the glucose concentration is linearly related to the glucose concentration in the range of 0.1-12 mM. The linear equation is $Current_{(mA/cm^2)} = 0.64086 + 0.27409C_{(mM)}$. The sensitivity of the Pt-Pd/Au sensor reaches 274.09 µA/cm^2/mM. This excellent detection sensitivity can be attributed to the large active surface area and pore volume of the nanowire array.

Table 1 shows the comparison between the sensing properties of Pt-Pd/Au with reported glucose sensors in literature. It is found from Table 1 that the sensitivity and detection limit of Pt-Pd/Au is better than other glucose sensors which indicating the more stability and more active electrochemical sites on nanostructured Pt-Pd surface.
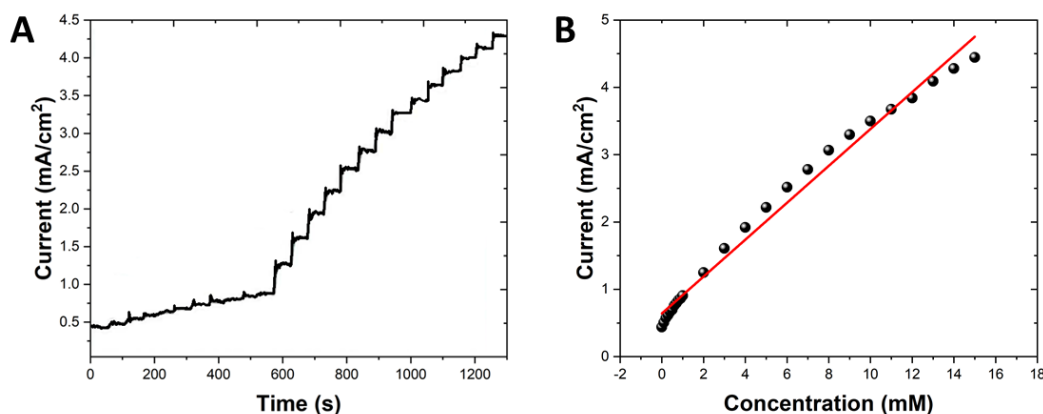
Figure 4. (A) Chronoamperometric response of the Pt-Pd/Au upon successive addition of glucose into 0.1 M PBS (pH 7.4). (B) Linear relationship of glucose concentration against the current density.

In general, electroactive substances present in the physiological environment such as 4-acetaminophen (AP), ascorbic acid (AA), dopamine (DA) and urea (UA) can also be oxidized at the electrode and cause interference [36–40]. Therefore, the interference resistance of glucose-free electrochemical sensors is one of the most important parameters to evaluate their performance. This study also investigated the immunity of the Pt-Pd/Au sensor to common interfering substances with the results shown in Figure 5. It is found that the amperometric response of the added interfering substance on the sensor is significantly lower than that of glucose, indicating that the sensor is highly selective for glucose.
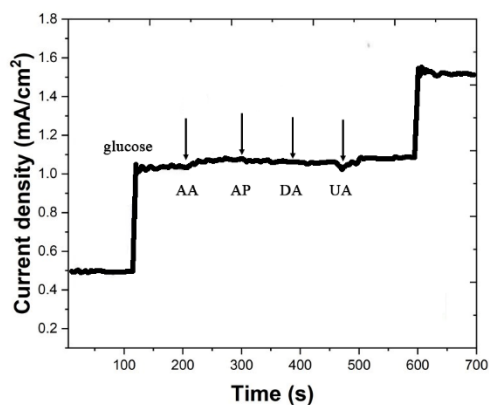
Figure 5. Chronoamperometric response of the Pt-Pd/Au upon successive addition of glucose, AP, AA, DA and UA.

Table 1. Comparison between the sensing properties of Pt-Pd/Au with reported glucose sensors in literatures.

Sensor	Linear range	Limit of detection	Ref.
Nano-SiO$_2$ film	0.005-2.5 mM	0.0003 μM	[41]
Glucose oxidase/graphene/chitosan nanocomposite	0.08-12 mM	0.02 μM	[42]
Chitosan-glucose oxidase composites/AuPt nanoparticles /rGO	0-2.4 mM	0.005 μM	[43]
SiO$_2$/GO/GCE	0-0.9 mM	0.03 μM	[44]
Pt-Pd/Au	0.1-12 mM	0.07 mM	This work

Table 2. Comparison of Pt-Pd/Au and biochemistry measurements.

Sample	Biochemical analyzer (mM)	Pt-Pd/Au (mM)	Deviation
1	2.25	-	-
2	3.24	3.17	-0.07
3	3.87	3.67	-0.20
4	4.66	4.69	0.03
5	8.21	8.32	0.11
6	9.55	9.57	0.02
7	9.97	9.91	-0.06
8	15.03	14.87	-0.16
9	18.55	18.67	0.12
10	18.31	18.20	-0.11

When the Pt-Pd/Au sensor is not used, it is stored dry at room temperature. The stability of the electrodes was tested by measuring the amperometric response to 10 mM glucose after the electrodes had been stored for a period of time. Three electrodes were prepared and tested at five-day intervals for 30 days. According to the experimental data, there is no significant decrease in the electrode's response to glucose at 10 days, a 2.2% decrease at 15 days, and a 7.7% decrease at 30 days, which indicates that the Pt-Pd/Au sensor has a good long-term stability.

10 serums with different glucose concentrations were measured with a Pt-Pd/Au sensor and a biochemical analyzer. The National Committee for Clinical Laboratory Standardization (NCCLS) published guidelines for the use of glucose POCT in 2002: for results greater than 4.2 mM, the difference between the POCT blood glucose meter and the central laboratory should be less than 20%; for results less than or equal to 4.2 mM, the difference is greater than or equal to 0.83 mM. Therefore, absolute deviations were calculated for glucose concentrations less than or equal to 4.2 mM, and relative deviations were calculated for concentrations greater than 4.2 mM. The results are shown in Table 2. The correlation coefficients of Pt-Pd/Au and biochemical analyzer for the first comparison are 0.991-0.998, which indicates that the correlation between Pt-Pd/Au and biochemical analyzer is excellent.

4. CONCLUSION

In this work, an enzyme-free glucose POCT electrochemical sensor based on Pt-Pd/Au was prepared. Pt-Pd was successfully prepared by a one-step electrodeposition method with an AAO template. The formation of Pt-Pd was controlled by both the electrodeposition rate and the diffusion rate of the solution in the AAO pore. The sensitivity of the Pt-Pd/Au sensor for glucose was 14.87 $\mu A/cm^2/mM$. The long-term stability of the sensor was proved to be good, and the sensitivity of glucose detection did not change significantly within 10 days.

References

1. S. Guo, C. Zhang, M. Yang, Y. Zhou, C. Bi, Q. Lv, N. Ma, *Anal. Chim. Acta*, 1109 (2020) 130–139.
2. L. Parashuram, S. Sreenivasa, S. Akshatha, V. Udayakumar, S. Sandeep kumar, *Food Chem.*, 300 (2019) 125178.
3. L. Fu, Z. Liu, J. Ge, M. Guo, H. Zhang, F. Chen, W. Su, A. Yu, *J. Electroanal. Chem.*, 841 (2019) 142–147.
4. R. Fu, Y. Lu, Y. Ding, L. Li, Z. Ren, X. Si, Q. Wu, *Microchem. J.*, 150 (2019) 104106.
5. W. Wu, Q. Zhou, Y. Zheng, L. Fu, J. Zhu, H. Karimi-Maleh, *Int J Electrochem Sci*, 15 (2020) 10093–10103.
6. D. Cheng, T. Wang, G. Zhang, H. Wu, H. Mei, *J. Alloys Compd.*, 819 (2020) 153014.
7. R. Duan, X. Fang, D. Wang, *Front. Chem.*, 9 (2021) 361.
8. H. Karimi-Maleh, Y. Orooji, F. Karimi, M. Alizadeh, M. Baghayeri, J. Rouhi, S. Tajik, H. Beitollahi, S. Agarwal, V.K. Gupta, *Biosens. Bioelectron.* (2021) 113252.
9. H. Karimi-Maleh, F. Karimi, S. Malekmohammadi, N. Zakariae, R. Esmaeili, S. Rostamnia, M.L. Yola, N. Atar, S. Movaghgharnezhad, S. Rajendran, A. Razmjou, Y. Orooji, S. Agarwal, V.K. Gupta, *J. Mol. Liq.*, 310 (2020) 113185.

10. J. Liu, T. Yang, J. Xu, Y. Sun, *Front. Chem.*, 9 (2021) 488.
11. Q. Liu, Y. Zheng, L. Fu, B.A. Simco, C.A. Goudie, *Aquaculture*, 532 (2021) 735952.
12. Y. Wang, X. Wang, W. Lu, Q. Yuan, Y. Zheng, B. Yao, *Talanta*, 198 (2019) 86–92.
13. N. Khalaf, T. Ahamad, M. Naushad, N. Al-hokbany, S.I. Al-Saeedi, S. Almotairi, S.M. Alshehri, *Int. J. Biol. Macromol.*, 146 (2020) 763–772.
14. J. Zhou, Y. Zheng, J. Zhang, H. Karimi-Maleh, Y. Xu, Q. Zhou, L. Fu, W. Wu, *Anal. Lett.*, 53 (2020) 2517–2528.
15. J. Li, S. Zhang, L. Zhang, Y. Zhang, H. Zhang, C. Zhang, X. Xuan, M. Wang, J. Zhang, Y. Yuan, *Front. Chem.*, 9 (2021) 339.
16. H. Karimi-Maleh, F. Karimi, L. Fu, A.L. Sanati, M. Alizadeh, C. Karaman, Y. Orooji, *J. Hazard. Mater.*, 423 (2022) 127058.
17. Y. Li, M. Xie, X. Zhang, Q. Liu, D. Lin, C. Xu, F. Xie, X. Sun, *Sens. Actuators B Chem.*, 278 (2019) 126–132.
18. L. Fu, A. Wang, G. Lai, W. Su, F. Malherbe, J. Yu, C.-T. Lin, A. Yu, *Talanta*, 180 (2018) 248–253.
19. H. Karimi-Maleh, M. Alizadeh, Y. Orooji, F. Karimi, M. Baghayeri, J. Rouhi, S. Tajik, H. Beitollahi, S. Agarwal, V.K. Gupta, S. Rajendran, S. Rostamnia, L. Fu, F. Saberi-Movahed, S. Malekmohammadi, *Ind. Eng. Chem. Res.*, 60 (2021) 816–823.
20. Q. Mei, R. Fu, Y. Ding, L. li, A. Wang, D. Duan, D. Ye, *J. Electroanal. Chem.*, 847 (2019) 113075.
21. Z. Wu, J. Liu, M. Liang, H. Zheng, C. Zhu, Y. Wang, *Front. Chem.*, 9 (2021) 208.
22. H. Karimi-Maleh, A. Ayati, R. Davoodi, B. Tanhaei, F. Karimi, S. Malekmohammadi, Y. Orooji, L. Fu, M. Sillanpää, *J. Clean. Prod.*, 291 (2021) 125880.
23. L. Fu, W. Su, F. Chen, S. Zhao, H. Zhang, H. Karimi-Maleh, A. Yu, J. Yu, C.-T. Lin, *Bioelectrochemistry* (2021) 107829.
24. X. Zhang, R. Yang, Z. Li, M. Zhang, Q. Wang, Y. Xu, L. Fu, J. Du, Y. Zheng, J. Zhu, *Rev. Mex. Ing. Quím.*, 19 (2020) 281–291.
25. Z. Xu, M. Peng, Z. Zhang, H. Zeng, R. Shi, X. Ma, L. Wang, B. Liao, *Front. Chem.*, 9 (2021) 683.
26. S. Yan, Y. Yue, L. Zeng, L. Su, M. Hao, W. Zhang, X. Wang, *Front. Chem.*, 9 (2021) 220.
27. T. Liu, Y. Guo, Z. Zhang, Z. Miao, X. Zhang, Z. Su, *Sens. Actuators B Chem.*, 286 (2019) 370–376.
28. J. Zhang, Y. Sun, X. Li, J. Xu, *J. Alloys Compd.*, 831 (2020) 154796.
29. W. Li, W. Luo, M. Li, L. Chen, L. Chen, H. Guan, M. Yu, *Front. Chem.*, 9 (2021) 610.
30. P. Chakraborty, S. Dhar, K. Debnath, S.P. Mondal, *J. Electroanal. Chem.*, 833 (2019) 213–220.
31. L. Fu, Q. Wang, M. Zhang, Y. Zheng, M. Wu, Z. Lan, J. Pu, H. Zhang, F. Chen, W. Su, *Front. Chem.*, 8 (2020) 92.
32. B. Fan, Q. Wang, W. Wu, Q. Zhou, D. Li, Z. Xu, L. Fu, J. Zhu, H. Karimi-Maleh, C.-T. Lin, *Biosensors*, 11 (2021) 155.
33. Y. Xu, Y. Lu, P. Zhang, Y. Wang, Y. Zheng, L. Fu, H. Zhang, C.-T. Lin, A. Yu, *Bioelectrochemistry*, 133 (2020) 107455.
34. B. Avinash, C.R. Ravikumar, M.R.A. Kumar, H.P. Nagaswarupa, M.S. Santosh, A.S. Bhatt, D. Kuznetsov, *J. Phys. Chem. Solids*, 134 (2019) 193–200.
35. C. Li, F. Sun, *Front. Chem.*, 9 (2021) 409.
36. A. Soleh, P. Kanatharana, P. Thavarungkul, W. Limbut, *Microchem. J.*, 153 (2020) 104379.
37. W. Long, Y. Xie, H. Shi, J. Ying, J. Yang, Y. Huang, H. Zhang, L. Fu, *Fuller. Nanotub. Carbon Nanostructures*, 26 (2018) 856–862.
38. Y. Zheng, H. Zhang, L. Fu, *Inorg. Nano-Met. Chem.*, 48 (2018) 449–453.
39. M. Zhang, B. Pan, Y. Wang, X. Du, L. Fu, Y. Zheng, F. Chen, W. Wu, Q. Zhou, S. Ding, *ChemistrySelect*, 5 (2020) 5035–5040.
40. J. Ying, Y. Zheng, H. Zhang, L. Fu, *Rev. Mex. Ing. Quím.*, 19 (2020) 585–592.

41. H. Yang, Y. Zhu, *Anal. Chim. Acta*, 554 (2005) 92–97.
42. X. Kang, J. Wang, H. Wu, I.A. Aksay, J. Liu, Y. Lin, *Biosens. Bioelectron.*, 25 (2009) 901–905.
43. X. Xuan, H.S. Yoon, J.Y. Park, *Biosens. Bioelectron.*, 109 (2018) 75–82.
44. W. Sun, S. Yu, J. Liu, Y. Ke, J. Sun, *Int. J. Electrochem. Sci.*, 16 (2021).